THE ASTROPHYSICAL JOURNAL, 342:934–939, 1989 July 15

WHAT IS CAUSING THE ECLIPSE IN THE MILLISECOND BINARY PULSAR?

FREDERIC A. RASIO, STUART L. SHAPIRO, AND SAUL A. TEUKOLSKY
Center for Radiophysics and Space Research, and Departments of Physics and Astronomy, Cornell University
Received 1988 June 21; accepted 1988 December 28

ABSTRACT

Possible physical mechanisms for explaining the radio eclipses in the millisecond binary pulsar PSR 1957+20 are discussed. If, as recent observations suggest, the duration of the eclipses depends on the observing frequency, a plausible mechanism is free-free absorption of the radio pulses by a low-density ionized wind surrounding the companion. We have performed detailed numerical calculations for this case, and find that all of the observations made at 430 MHz can be reliably reproduced, including the asymmetry in the excess time delay of the pulses. Our model leads to definite predictions for the duration of the eclipse at other observing frequencies, as well as the radio intensity and excess time delay of the pulses as a function of orbital phase.

If the duration of the eclipses were found to be independent of frequency, then the likely mechanism would be reflection of the radio signal at a contact discontinuity between a high-density wind and the pulsar radiation. In this case, however, it is difficult to explain the observed symmetry of the eclipse.

Subject headings: pulsars — radiation mechanisms — stars: eclipsing binaries — stars: radio radiation

I. INTRODUCTION

The very exciting discovery of a new millisecond pulsar, PSR 1957+20, in an eclipsing low-mass binary, was recently announced by Fruchter, Stinebring, and Taylor (1988). Given the orbital parameters of the system, and assuming a neutron star mass $m_p = 1.4\ M_\odot$ and $\sin i = 1$ in the mass function,

$$f(m_p, m_c) \equiv \frac{(m_c \sin i)^3}{(m_p + m_c)^2} = 5.2 \times 10^{-6}\ M_\odot\ , \qquad (1)$$

we deduce a companion mass $m_c = 0.02\ M_\odot$ and binary separation $a = 2.4\ R_\odot$. The pulsar period, $P = 1.61$ ms, is very close to that of PSR 1937+21 ($P = 1.56$ ms; see Backer *et al.* 1982), suggesting a comparable spin-down power $L \approx 2 \times 10^{36}$ ergs s^{-1} (see, e.g., Ashworth, Lyne, and Smith 1983).

At 430 MHz, radio eclipses are observed between orbital phases $\phi = 0.21$ and $\phi = 0.29$, where orbital phase ϕ is measured from the time of the ascending node. The eclipse interval is therefore very nearly symmetric about $\phi = 0.25$, corresponding to the moment when the pulsar is directly behind the companion. However, the observed excess time delay of the pulses appears very asymmetric, rising very steeply before the leading edge of eclipse, but decreasing much more slowly after the trailing edge.

As pointed out by several authors (Fruchter *et al.* 1988; Kluźniak *et al.* 1988; Phinney *et al.* 1988), the duration of the eclipses observed at 430 MHz implies that the radius of the eclipsing region $r_E = 0.7\ R_\odot$ greatly exceeds the Roche lobe of the companion ($r_{\rm Roche} \approx 0.3\ R_\odot$). This indicates the presence of a stellar wind surrounding the companion. Such a wind results from the interaction of the companion with a high-energy component of the pulsar radiation (Ruderman, Shaham, and Tavani 1988; Kluźniak *et al.* 1988). If the resulting mass loss rate is large enough, the companion could eventually be completely evaporated, leaving behind an isolated millisecond pulsar like PSR 1937+21. The deflection of the wind due to the combined effects of radiation pressure and Coriolis forces may explain the asymmetry in excess time delay of the radio pulses.

In this paper, we discuss possible physical mechanisms by which this wind can eclipse the radio signals from the pulsar. Central to our discussion is the decomposition of the pulsar radiation (at the moment when it reaches the wind) into three components: (1) radiation that is either absorbed or reflected by an ionized wind and therefore exerts pressure on it (typically this could be low frequency [kHz] electromagnetic radiation); (2) radiation that propagates through the wind without being significantly absorbed or scattered (typically this could be a high-energy flux of Mev to GeV γ-rays and TeV $e^\pm$); and (3) the radio component per se, which clearly is at least partially absorbed as it propagates through the wind. The radio component is known to represent only a very small fraction (typically $\sim 10^{-6}$) of the total spin-down power, but it is uncertain whether the rest is mainly in the form of type 1 or type 2 radiation (Ruderman *et al.* 1988, however, argue that type 2 is likely to be the major component in a system such as this one). Prior to reaching the companion, most radiation of type 1 could get transformed into type 2 as it propagates out through the pulsar magnetosphere. The interaction of type 2 radiation with the outer layers of the companion is what excites the wind.

In § II, we present a model based on *free-free absorption* of the radio pulses as they propagate through the wind. This model requires that the nonradio pulsar luminosity *interact negligibly* with the wind, i.e., that it be mainly of type 2 (high-energy γ-rays and $e^\pm$) by the time it reaches the wind. We refer to this as the "optically thin" case, for which we have performed detailed numerical calculations of the wind structure. In § III, an alternative and radically different model is discussed, in which the radio pulses are *reflected* away from the eclipsing region. Here, on the contrary, the wind *must be mostly opaque* to the radiation from the pulsar, implying that the pulsar radiation be still largely of type 2 (low-frequency electromagnetic radiation) when it reaches the wind. We refer to this as the "optically thick" case.

II. OPTICALLY THIN WIND

In this section, we will determine the properties of the wind assuming complete ionization, and *free-free absorption* of the

radio signals as the eclipsing mechanism. As we will show, this implies a rather low wind density $\rho \approx 10^{-18}$ g cm^{-3}. It is easy to see why such a low density in turns requires that only a small fraction of the pulsar radiation be in a form that can exert pressure on the wind, such as low-frequency electromagnetic radiation. If fL_p is the fraction of the pulsar luminosity L_p that exerts pressure on the wind, this pressure can be written (assuming isotropy for simplicity) $P_{\rm rad} \approx fL_p/(4\pi a^2 c)$, where a is the binary separation, and c is the speed of light. The ram pressure in the wind on the other hand can be written $P_{\rm wind} \approx \rho v_w^2$, where the wind velocity v_w is of the order of the orbital velocity. Momentum balance then requires $P_{\rm rad} = P_{\rm wind}$, which gives a very small f:

$$f \approx 10^{-4}\left(\frac{\rho}{10^{-18}\ \mathrm{g\ cm^{-3}}}\right)\left(\frac{v_w}{1000\ \mathrm{km\ s^{-1}}}\right)^2 \times \left(\frac{L_p}{10^{36}\ \mathrm{ergs\ s^{-1}}}\right)^{-1} . \quad (2)$$

a) *A Simple Analytical Model*

We first construct a simple analytical model, assuming spherical symmetry about the companion (i.e., neglecting Coriolis and centrifugal forces), and a constant velocity, fully ionized wind. Since mass conservation implies $n_e(r)v_w \times 4\pi r^2 = \text{const}$, where $n_e(r)$ is the electron number density at a distance r from the center of the companion, we get

$$n_e(r) = n_e(r_E)(r_E/r)^2 . \quad (3)$$

This picture is justified if the wind acquires a velocity sufficiently large compared to the orbital velocity.

For the temperature in the wind, we assume $T \propto n_e^{\gamma-1}$, where γ is a constant. This, with equation (3), yields a simple power-law profile

$$T(r) = T(r_E)(r_E/r)^{2(\gamma-1)} . \quad (4)$$

This form, parameterized by an unknown quantity γ, reflects our uncertainties regarding heating and cooling in the system. Indeed, the chemical composition of the wind (especially its metallicity), as well as the composition of the pulsar radiation are essentially unknown to us at the present time. In what follows, we will consider for definiteness two extreme cases, namely, $\gamma = 1$, which corresponds to an "isothermal wind," and $\gamma = 5/3$, which is appropriate for an adiabatically cooling wind.

With these assumptions concerning the density and temperature of the wind, the free-free absorption coefficient at frequency ν can be written (see, e.g., Spitzer 1978)

$$\kappa_\nu = \frac{(0.173\ \mathrm{cm^{-1}})Z^2 g(\nu, T) n_e^2(r_E)}{T^{3/2}(r_E)\nu^2}\left(\frac{r_E}{r}\right)^{7-3\gamma} , \quad (5)$$

where the Gaunt factor $g(\nu, T) = 1 + 0.13 \log (T^{3/2}/\nu)$, and Z is the atomic number of the dominant species (or the average net charge per atom if the gas is not fully ionized). Integrating κ_ν along the line of sight gives the optical depth τ_ν. For an isothermal wind we find

$$\tau_\nu = \frac{(0.173\ \mathrm{cm^{-1}})Z^2 \bar{g} n_e^2(r_E)}{T^{3/2}(r_E)\nu^2}\left(\frac{r_E^4}{a^3}\right)J(\theta) \quad (\gamma = 1) , \quad (6)$$

where

$$J(\theta) \equiv \frac{1}{2\sin^2\theta}\left(\cos\theta + \frac{\pm\pi - \theta}{\sin\theta}\right) \quad \text{for } \theta \gtrless 0 , \quad (7)$$

and $\bar{g} \approx 1 + 0.13 \log [T^{3/2}(r_E)/\nu]$. Here $\theta \equiv 2\pi(0.25 - \phi)$ is the angle between the line of sight and the direction corresponding to orbital phase $\phi = 0.25$ (i.e., the center of the eclipse). For an adiabatically cooling wind, equation (6) is replaced by

$$\tau_\nu = \frac{(0.173\ \mathrm{cm^{-1}})Z^2 \bar{g} n_e^2(r_E)}{T^{3/2}(r_E)\nu^2}\left(\frac{r_E^2}{a}\right)I(\theta) \quad \left(\gamma = \frac{5}{3}\right) , \quad (8)$$

where now

$$I(\theta) \equiv \frac{1}{\sin\theta}(\pm\pi - \theta) \quad \text{for} \quad \theta \gtrless 0 . \quad (9)$$

Equation (6), or equation (8), determines the expected light curve at frequency ν, up to a normalization. At $\nu = 430$ MHz, this normalization is easily obtained [independent of any specific values adopted for a, $n_e(r_E)$, or $T(r_E)$] by requiring that $\tau_\nu \approx 1$ when $\phi = 0.21$, or $\phi = 0.29$, as observed.

Had we neglected the very small frequency dependence of the Gaunt factor $\bar{g}$, light curves for other frequencies (Fig. 1) would be directly obtained from the $1/\nu^2$ dependence of τ_ν. However, a complete normalization follows naturally from considering the observed excess time delay of the signals. Integrating $n_e(r)$ along the line of sight gives the dispersion measure

$$DM = n_e(r_E)\left(\frac{r_E^2}{a}\right)I(\theta) . \quad (10)$$

Then by requiring that, for $\nu = 430$ MHz, the excess time delay $\Delta t_a = (e^2/2\pi m_e c)DM/\nu^2$ of the pulses received at $\phi = 0.30$ be equal to the observed 350 μs, we obtain from equation (10) $n_e(r_E) = 0.47 \times 10^6$ cm^{-3}, in agreement with a preliminary estimate by Fruchter *et al.* (1988). Finally, we set $\tau_\nu = 1$ for $\nu = 430$ MHz and $\phi = 0.21$ in equations (6) and (8), and get $T(r_E) = 300\ \mathrm{K}\ Z^{4/3}$ for $\gamma = 1$ and $T(r_E) = 450\ \mathrm{K}\ Z^{4/3}$ for $\gamma = 5/3$.

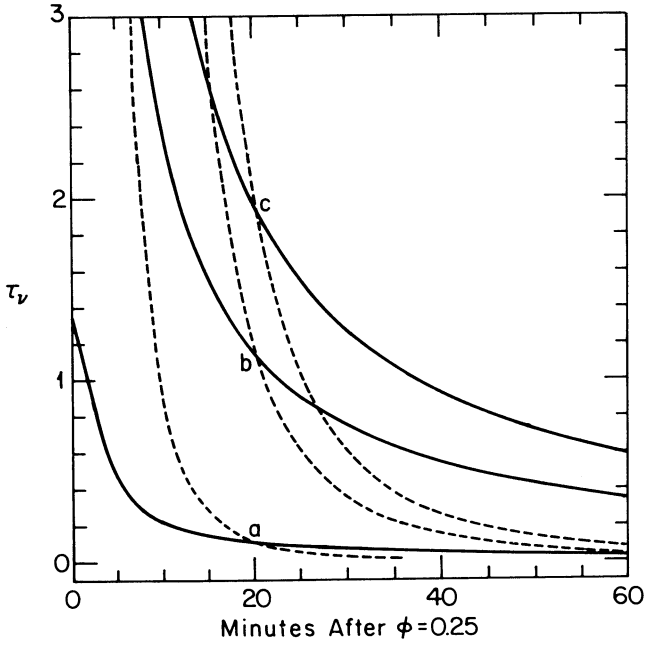

FIG. 1.—Frequency dependent light curves [$I_\nu = I_\nu^{\rm ac} \exp(-\tau_\nu)$] expected from free-free absorption. Solid lines are for an adiabatically cooling wind, dashed lines for an isothermal wind. Curves labeled *a*, *b*, and *c* correspond to $\nu = 1408$ MHz, 430 MHz, and 316 MHz, respectively.

It is interesting to note that the adiabatic case ($\gamma = 5/3$) predicts a temperature $T(r_c) \approx T(r_E)(r_E/r_c)^{4/3} \approx 3500\ \mathrm{K}\ Z^{4/3}$ at the surface of the companion (estimated to be at $r_c \approx 0.15\ R_\odot$ for a $0.02\ M_\odot$ degenerate dwarf, assuming $Z \approx 1$; see, e.g., Shapiro and Teukolsky 1983), in agreement with a recent optical observation of the companion by Kulkarni, Djorgovski, and Fruchter (1988).

As pointed out by Wasserman and Cordes (1988), the low values obtained for $T(r_E)$ do not necessarily imply a low ionization fraction here, since the recombination time is much larger than any typical crossing time. Note also that the wind itself will not radiate X-rays or γ-rays. For a completely ionized wind and $Z = 1$, the mass density $\rho(r_E) = 0.8 \times 10^{-18}\ \mathrm{g\ cm^{-3}}$. The corresponding mass loss rate from the companion $\dot{m}_c = 4\pi r_E^2 \rho(r_E) v \approx 10^{-13}\ M_\odot\ \mathrm{yr}^{-1}$, implying a characteristic lifetime $t_c \equiv m_c/\dot{m}_c \approx 10^{11}$ yr, longer than the age of the universe. However, different orbital parameters could easily lead to shorter lifetimes, as required to explain the disappearance of the companion in systems like PSR 1937+21.

The most important consequence of this model is that *the duration of the observed radio eclipses should be a sensitive function of frequency*. In particular, in the limit of large frequencies, $\theta \ll 1$ in equations (7) and (9), so that equations (6) and (8) predict that the duration of the eclipses should vary like $\nu^{-2/3}$ for an isothermal wind, and like ν^{-2} for an adiabatically cooling wind. An observed duration of the eclipses varying like $\nu^{-\alpha}$ with $\alpha < 2/3$ could indicate a significant net heating of the wind, whereas $\alpha > 2$ could indicate a significant net cooling. At present, *there is* preliminary evidence for a frequency dependence of the eclipse duration (from recent observations at 318 MHz; J. Taylor, private communication), but the slope of the variation has not yet been determined. It appears, however, that the duration does indeed increase with decreasing frequency. Table 1 summarizes the key predictions that follow from equations (6)–(10). Note that the maximum measureable excess time delay increases with frequency for $\gamma = 5/3$, but decreases for $\gamma = 1$. This can be understood if one remembers that increasing the frequency lowers the time delay, but at the same time allows higher density regions to become visible, thereby increasing the maximum dispersion measure.

b) *A Numerical Model for the Asymmetry in Excess Time Delay*

The simple analytical model presented above was built on the assumption that the wind can be well enough represented by a spherically symmetric density profile near the companion. However, even though the eclipse itself appears symmetric at 430 MHz, the excess time delay of the pulses decreases much more slowly on the trailing edge than on the leading edge of eclipse. The only way to get such an asymmetry is to allow the transonic wind velocity in the model to decrease to the point where it becomes comparable to the orbital velocity. At that point all the forces in the system (gravitational, Coriolis, centrifugal, radiation pressure) must be taken into account to determine the structure of the plasma flow. In particular the combined actions of radiation pressure from the pulsar emission and the Coriolis force will tend to force the wind into a narrow trailing tail of plasma, as in a comet near perihelion (Fig. 2).

TABLE 1

FREQUENCY DEPENDENCE OF THE ECLIPSES PRODUCED BY FREE-FREE ABSORPTION

Observing Frequency (MHz)	Eclipse Duration[a] (minutes)		Maximum Measurable[b] Excess Time Delay	
	$\gamma = 1$	$\gamma = 5/3$	$\gamma = 1$	$\gamma = 5/3$
111	120	∞	2200	...
318	56	81	630	420
430	44	44	450	450
609	34	22	290	460
1408	19	3.3	100	600

[a] For comparison, the orbital period $P = 550$ minutes.
[b] Calculated at the orbital phase where $\tau_\nu = 1$.

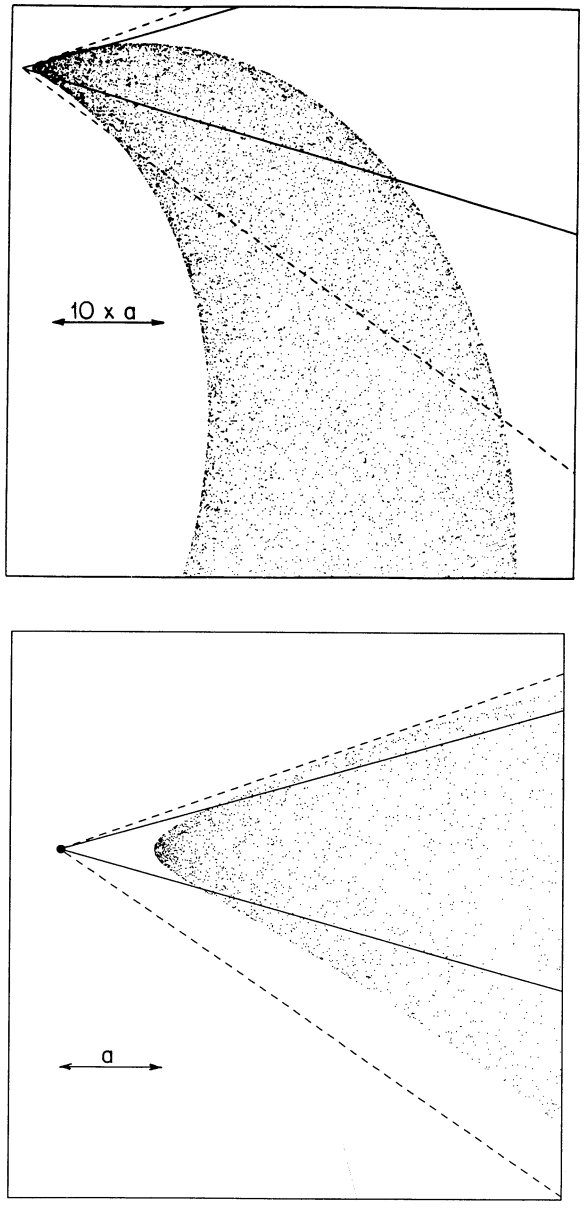

FIG. 2.—(*a*) Structure of an optically thin wind, in the orbital plane, as determined by our particle simulation. The positions (*dots*) of only a few thousand particles are shown. Four critical lines of sight have been indicated: the two solid lines show the observed position of the radio eclipse at 430 MHz, whereas the two dashed lines indicate where an excess time delay appears, or disappears, for the first time before or after eclipse respectively (in the data of Fruchter *et al.* 1988). (*b*) Detail of the region near the neutron star, indicated by a large dot. Note that the radiation pressure evacuates the wind from the region near the pulsar, preventing accretion.

An analytic treatment of this is clearly impossible. Our numerical calculations are based on the following two simplifying assumptions: (1) Internal pressure in the wind is negligible, i.e., the wind flow is highly supersonic. (2) The radiation pressure can be computed assuming as before that the radiation from the pulsar is only partially absorbed by an optically thin gas. Assumption 1 implies that fluid elements in the wind follow ballistic trajectories. This allows us to use *free particle simulations*, integrating numerically the equations of motion of a large number of representative test particles and determining the local density by binning the particles. Assumption 2 implies that we can compute the radiation force on each individual particle as $\boldsymbol{F}_{\rm rad} = -C_{\rm rad}\boldsymbol{F}_{\rm grav}$, where $C_{\rm rad}$ is a constant and $\boldsymbol{F}_{\rm grav}$ is the gravitational attraction of the neutron star (clearly, $C_{\rm rad} > 1$ since there is no pulsar accretion). It is important to note that *no assumption concerning the temperature structure of the wind is needed here, since the excess time delay depends only on the wind density profile.*

In the simulations, we eject particles isotropically, at a constant rate from the surface of the companion, at $r_c = 0.15\ R_\odot$. By a numerical coincidence, this makes the escape velocity from the companion ($v_{\rm esc} \approx 220$ km s^{-1}) comparable to the orbital velocity $v_{\rm orb} = 340$ km s^{-1}. Our results, however, are not sensitive to the adopted value of r_c, since the gravitational forces turn out to be dominated by radiation. In units such that $a = M = \omega = 1$, where M is the total mass of the system and ω the orbital frequency, the equations of motion of a wind particle in the corotating frame can be written:

$$\dot{x} = -(1 - C_{\rm rad})(1 - \mu)\frac{(x + \mu)}{d^3} - \mu\frac{(x + \mu - 1)}{r^3} + 2\dot{y} + x\,, \tag{11}$$

$$\dot{y} = -(1 - C_{\rm rad})(1 - \mu)\frac{y}{d^3} - \mu\frac{y}{r^3} - 2\dot{x} + y\,, \tag{12}$$

$$\dot{z} = -(1 - C_{\rm rad})(1 - \mu)\frac{z}{d^3} - \mu\frac{z}{r^3}\,. \tag{13}$$

Here $\mu \equiv m_c/(m_p + m_c)$, $d = [(x + \mu)^2 + y^2 + z^2]^{1/2}$ is the distance to the neutron star, and $r = [(x - 1)^2 + y^2 + z^2]^{1/2}$ is the distance to the companion. The origin of our coordinate system is at the center of mass of the binary, the x-axis joins the neutron star to the companion, and the z-axis is perpendicular to the orbital plane. Equations (11)–(13) are integrated using a fifth-order self-adaptive Runge-Kutta scheme (see, e.g., Press *et al.* 1986). Once a very large number of particles (typically 10^5) have been moved, column density and opacity are computed (up to a normalization) by binning the particles and using the trapezoidal rule to integrate along the line of sight. A useful test-bed calculation consists in running the simulation for a high-velocity wind and checking that the analytic results discussed above are recovered.

The ejection velocity $v_{\rm ejec}$ and the constant $C_{\rm rad}$ are the only free parameters in the model. They were determined by fitting the predicted excess time delay to the observations. In particular, the slope of the decreasing part of the curve and the point at which it starts rising are sensitive functions of both parameters. Our best fit corresponds to $C_{\rm rad} = 1.2 \times 10^3$ and $v_{\rm ejec} = 15v_{\rm sec} = 10v_{\rm orb}$, which are readily determined to within 20%. As shown in Figure 3, the asymmetry is almost perfectly reproduced. As noted above, it is important to realize that this result does not depend on any particular assumption concerning the thermal structure of the wind (which is one of the biggest unknowns in this problem), except for the general requirement that the flow remains everywhere supersonic.

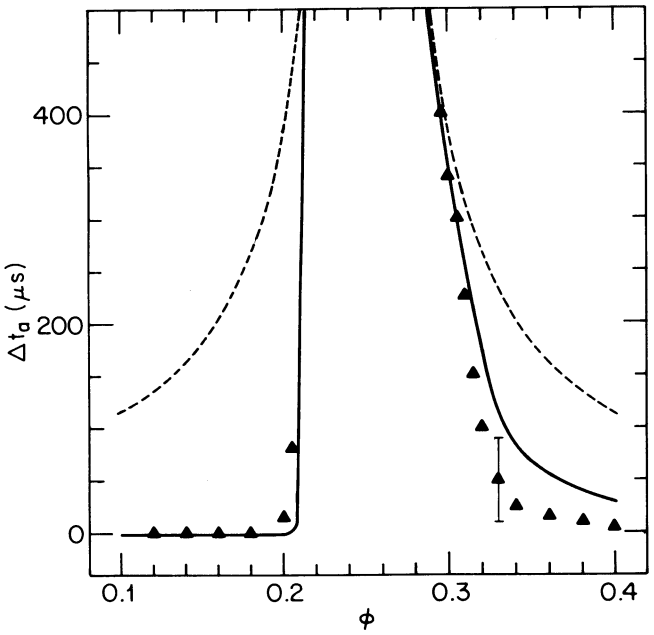

FIG. 3.—Excess time delay in the pulsar signal at 430 MHz, plotted as a function of orbital phase near the center of eclipse. Dashed line is from the simple (spherically symmetric) analytical model of free-free absorption, solid line is the best fit from our particle simulation. Filled triangles correspond to measured values (from Fruchter *et al.* 1988). The error bar indicates the typical scatter in the data.

c) *Constraints on the Pulsar Radiation*

Interestingly, the value of $C_{\rm rad}$ derived above from dynamical considerations can also be obtained directly by assuming that *radio waves alone* deflect the wind. Indeed, in this case the radiation force per baryon in the wind, at a distance d from the pulsar (assuming isotropy), can be written

$$F_{\rm rad}(d) = \frac{1}{4\pi c}\int_{\nu_c}^{\infty} \mathscr{F}_\nu(d)\left(\frac{\nu_c}{\nu}\right)^2 \sigma_\nu\, d\nu\,, \tag{14}$$

where $\mathscr{F}_\nu(d)$ is the radio flux density (ergs cm^{-2} s^{-1} Hz^{-1}) at a distance d from the pulsar, $\sigma_\nu = \kappa_\nu/n_e$ (see eq. [5]) is the effective cross section for free-free absorption, and we have assumed a radio spectrum with spectral index ≈ -2 and a lower frequency cutoff at $\nu_c \approx 10$ MHz, by analogy with PSR 1937+21 (see, e.g., Erickson and Mahoney 1985). We now relate $\mathscr{F}_\nu(d)$ to the flux density $\mathscr{F}_\nu(D)$ measured at the Earth by $\mathscr{F}_\nu(d) = \mathscr{F}_\nu(D)(D^2/d^2)$, where D is the distance from the Earth to the pulsar, estimated to be ≈ 1 kpc given the dispersion measure $DM \approx 30$ pc cm^{-3}. Equation (14) then implies a constant value of $C_{\rm rad} \equiv F_{\rm rad}(d)/(Gm_p m_B/d^2)$ (where m_B is the mass of a baryon) very close to what we found numerically:

$$C_{\rm rad} = 2.2 \times 10^3 Z^2\left(\frac{m_p}{1.4\ M_\odot}\right)^{-1}\left(\frac{n_e}{10^6\ {\rm cm}^{-3}}\right)\left(\frac{T}{100\ {\rm K}}\right)^{-3/2} \times \left(\frac{\nu_c}{10\ {\rm MHz}}\right)^{-1}\left(\frac{\mathscr{F}_{\nu_c}(D)}{10^3\ {\rm Jy}}\right)\left(\frac{D}{1\ {\rm kpc}}\right)^2\,. \tag{15}$$

Note that for an adiabatically cooling wind, $n_e/T^{3/2} = n_e(r_E)/T^{3/2}(r_E) =$ constant, but for an isothermal wind, n_e in equation (15) is a suitably averaged quantity.

If additional sources of pressure were present, a low-density optically thin wind would be swept back entirely, leaving an eclipsing region much smaller than observed. *The validity of this optically thin model therefore puts a strong constraint on the composition of the pulsar radiation.* Specifically, we can write the condition that all particle and radiation (other than radio) fluxes from the pulsar do not transfer any appreciable momentum to the wind, in one crossing time, as

$$\frac{1}{4\pi a^2 c}\int L_\epsilon \sigma_\epsilon \, d\epsilon\left(\frac{r_E}{v_w}\right) < m_B v_w \, . \tag{16}$$

Here L_ϵ is the nonradio luminosity per unit energy ϵ, absorbed by one baryon with a characteristic cross section σ_ϵ. Defining a mean cross section for energy-momentum transfer $\bar{\sigma} \equiv L_p^{-1}\int L_\epsilon \sigma_\epsilon \, d\epsilon$, where $L_p = \int L_\epsilon \, d\epsilon$, we find that equation (16) implies

$$\bar{\sigma} < 5 \times 10^3 \sigma_T \left(\frac{L_p}{10^{36}\ \mathrm{ergs\ s^{-1}}}\right)^{-1}\left(\frac{v_w}{1000\ \mathrm{km\ s^{-1}}}\right)^2 , \tag{17}$$

where σ_T is the Thomson cross section. This inequality essentially requires again that most of the low-frequency electromagnetic radiation emitted by the pulsar be transformed into high-energy particles and photons (which all have cross sections $\sigma \lesssim 0.01\sigma_T$) over a distance $d < a$.

Even more severe constraints can in principle be obtained by modeling heating and cooling in the wind. For example, if cooling is totally negligible, then the rather low wind temperatures required for free-free absorption to be effective can be maintained only if heating is also completely negligible. This condition can be written in a form similar to (16), as

$$\frac{1}{4\pi a^2}\int L_\epsilon \sigma_\epsilon \, d\epsilon\left(\frac{r_E}{v_w}\right) < 3kT(r_E) \, , \tag{18}$$

which is equivalent to reducing the numerical coefficient in equation (17) by $[3kT(r_E)/m_B v_w^2] \times (v_w/c) \sim 10^{-6}$ (For the radio emission itself the condition is marginally violated at $r \sim r_E$). However, efficient cooling mechanisms in the eclipsing region could very well be present. To mention only a few, magnetic fields could be strong enough in the eclipsing region ($\gtrsim 100$ G, see Kluźniak *et al.* 1988) to make cyclotron emission important. Cooling by inelastic collisions could be important since the wind is formed by the evaporation of an evolved star and could therefore have a very high metallicity. We feel that a detailed treatment of all this is not possible at present given the lack of observational data.

III. OPTICALLY THICK WIND

In § II we have implicitly assumed that the plasma frequency in the wind,

$$\nu_p = 9.3\ \mathrm{MHz}\left(\frac{n_e}{10^6\ \mathrm{cm^{-3}}}\right)^{1/2} , \tag{19}$$

was everywhere below the observing frequency $\nu > \nu_c \approx 100$ MHz. This condition is clearly satisfied for an optically thin wind where $n_e \approx 10^6$ cm^{-3}. We now explore the alternative possibility of having an optically thick wind, which completely blocks most of the radiation from the pulsar. We can roughly estimate the density ρ in the wind by writing momentum balance as $\rho v_w^2 \approx L_p/(4\pi a^2 c)$. This gives

$$\rho \approx 10^{-14}\ \mathrm{g\ cm^{-3}}\left(\frac{L_p}{10^{36}\ \mathrm{erg\ s^{-1}}}\right)\left(\frac{v_w}{1000\ \mathrm{km\ s^{-1}}}\right)^{-2} . \tag{20}$$

For a completely ionized wind, this value implies an electron number density $n_e \approx 10^{10}$ cm^{-3}. From equation (19), we see that in this case *the radio pulses cannot propagate through the wind at all.* Moreover, since the electron number density just outside the eclipsing region, estimated from the dispersion measure, is only $\approx 10^5$ cm^{-3}, *the wind must be bounded by a sharp contact discontinuity.*

This opaque model has been discussed recently by Phinney *et al.* (1988). Its most immediate consequence is that *the duration of the radio eclipses should be independent of observing frequency* (since all frequencies below ν_p are equally blocked on the same surface of discontinuity), which does not seem to be the case (see discussion in § II*a*). Moreover, in such a picture, it is hard to understand how the eclipse would appear perfectly symmetric about orbital phase $\phi = 0.25$, as observed, unless the region filled by the wind itself is symmetric with respect to the line joining the companion to the neutron star. For any wind velocity comparable to the orbital velocity, this is very unlikely since Coriolis forces tend to deflect the wind backwards. The large mass density of equation (20) also implies a short lifetime for the companion, $t_c \approx 10^7$ yr. While such a short lifetime could explain the disappearance of the companion in a system like PSR 1937+21, one could argue that a short lifetime also makes the probability of discovering a system like the present one very low.

As pointed out by Wasserman and Cordes (1988), the large mass density derived from momentum balance does not necessarily imply a correspondingly large electron number density, since it is not possible, *a priori*, to rule out a low ionization fraction in the wind. The low electron number density of § II, obtained by assuming that eclipses are produced by free-free absorption, can be reconciled with the large mass density of equation (19) if the ionization fraction in the gas $\chi \approx 10^{-4}$. The presence of a contact discontinuity is therefore not incompatible with free-free absorption being the dominant eclipsing mechanism. However, it is difficult to imagine that the gas would remain unionized when the temperature and density rise sharply at the discontinuity.

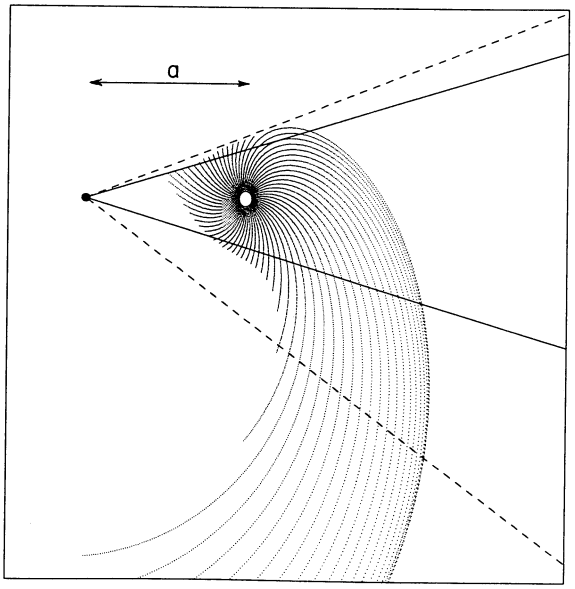

FIG. 4.—Structure of an optically thick wind. The trajectories end abruptly at a contact discontinuity, where momentum balance is established between the wind and the pulsar radiation. Notations are as in Fig. 2.

Quite apart from the ionization state of the wind, the shape of the discontinuity can be determined in first approximation by generalizing the momentum balance argument given above. We used the following procedure. As before, we integrate the equations of motion (11)–(13) numerically to determine stream lines of the wind in the orbital plane, neglecting internal pressure. Along each trajectory, we compute the quantity

$$\delta \equiv \left(\frac{S_0}{S}\right)\left(\frac{v}{v_0}\right)\left(\frac{d}{a}\right)^2 = \frac{\rho v^2}{\rho_0 v_0^2}\left(\frac{d}{a}\right)^2, \tag{21}$$

where S is the cross-sectional area of a stream tube, determined from neighboring trajectories, and a subscript 0 indicates a value at the surface of the companion. The trajectory stops when momentum balance is established, i.e., when δ becomes equal to the critical value

$$\delta_{\rm crit} = \frac{L}{12\pi a^2 c \rho_0^2 v_0^2}, \tag{22}$$

obtained by setting $\rho v^2 = (1/3)L/(4\pi d^2 c)$ in equation (21), the factor (1/3) assuming an isotropic radiation pressure outside the wind. The two free parameters in the calculation are $\delta_{\rm crit}$ and v_0. If we assume that free-free absorption is still dominant (and therefore that the ionization fraction in the wind is low), the parameters can be determined as before, by fitting the predicted excess time delay to the observations. Figure 4 shows the geometry of the wind for our best fit, corresponding to $\delta_{\rm crit} = 0.13$ and $v_0 = 1.2 v_{\rm orb}$. The results of Table 1 again apply in this special case. However, our results here should be considered very crude preliminary calculations of a problem which clearly would require more sophisticated three-dimensional hydrodynamical modeling.

We thank D. Stinebring and J. Taylor for discussing observations in progress, I. Wasserman and J. Cordes for useful discussions and communicating results prior to publication, and L. Bildsten and D. Chernoff for valuable conversations. We acknowledge support from NSF grants AST 87-14475 and PHY 86-03284 to Cornell University.

REFERENCES

Ashworth, M., Lyne, A. G., and Smith, F. G. 1983, *Nature*, **301**, 313.
Backer, D. C., Kulkarni, S. R., Heiles, C., Davis, M. M., and Goss, W. M. 1982, *Nature*, **300**, 615.
Erickson, W. C., and Mahoney, M. J. 1985, *Ap. J. (Letters)*, **299**, L29.
Fruchter, A. S., Stinebring, D. R., and Taylor, J. H. 1988, *Nature*, **333**, 237.
Kluźniak, W., Ruderman, M., Shaham, J., and Tavani, M. 1988, *Nature*, **334**, 225.
Kulkarni, S. R., Djorgovski, S., and Fruchter, A. S. 1988, *Nature*, **334**, 504.
Phinney, E. S., Evans, C. R., Blandford, R. D., and Kulkarni, S. R. 1988, *Nature*, **333**, 832.
Press, W. H., Flannery, B. P., Teukolsky, S. A., and Vetterling, W. T. 1986, *Numerical Recipes* (Cambridge: Cambridge University Press).
Ruderman, M., Shaham, J., and Tavani, M. 1989, *Ap. J.*, submitted.
Shapiro, S. L., and Teukolsky, S. A. 1983, *Black Holes, White Dwarfs, and Neutron Stars* (New York: Wiley).
Spitzer, L. 1978, *Physical Processes in the Interstellar Medium* (New York: Wiley).
Wasserman, I., and Cordes, J. M. 1988, *Ap. J. (Letters)*, **333**, L91.

FREDERIC A. RASIO, STUART L. SHAPIRO, and SAUL A. TEUKOLSKY: Cornell University, Space Sciences Building, Ithaca, NY 14853